Applied Radiation and Isotopes 206 (2024) 111243

Contents lists available at ScienceDirect

Applied Radiation and Isotopes

journal homepage: www.elsevier.com/locate/apradiso

Emission characteristics of pulse CNT cold cathode X-ray source combined with channel electron multiplier

Kai Miao [a,c], Yunpeng Liu [a,b,*], Sheng Lai [a], Junqiu Yin [a], Feixu Xiong [a], Xiaoyu Dong [a,c], Xiaobin Tang [a,b,**]

[a] Department of Nuclear Science and Technology, Nanjing University of Aeronautics and Astronautics, Nanjing, 210016, China
[b] Key Laboratory of Nuclear Technology Application and Radiation Protection in Astronautics, Ministry of Industry and Information Technology, Nanjing, 210016, China
[c] IRay Electric Vacuum Technology (Nanjing) Co., Ltd., Nanjing, 210016, China

ARTICLE INFO

Keywords:
High-frequency pulse X-ray source
CNT field emission
Channel electron multiplier
DC characteristics
Pulse characteristics

ABSTRACT

Carbon nanotube (CNT)-based field emission X-ray source with the advantage of fast start-up response offers the chance to achieve high-frequency X-ray emission. In this study, a high-frequency random pulse X-ray source of CNT cold cathode combined with a channel electron multiplier (CEM) was built, and its direct current (DC) and pulse emission characteristics were tested. The DC measurement results were used for parameter selection for performing pulse experiments. During the DC test, with the conditions of 2.2 kV CEM bias voltage and 25 kV anode voltage, the anode currents are 141, 250, and 300 μA at grid voltages of 290, 387.6, and 432.2 V, respectively; the corresponding grid field values are 1.45, 1.94, and 2.16 V/μm. During the pulse test, the amplitude–frequency response of the X-ray source reaches 3.58 MHz at 3 dB. The developed pulse X-ray source was introduced into the X-ray communication (XCOM), and the experimental communication rate reached 6 Mbps with the bit-error-rate of 1.1×10^{-3}. The developed high-frequency pulse CNT-CEM X-ray source has potential applications in XCOM, high-speed X-ray imaging, and other fields.

1. Introduction

X-ray communication (XCOM) is a type of high-speed space communication method that utilizes pulse X-rays with random waveforms as carriers for effective data transmission. The X-ray sources in XCOM rely on random signals instead of repetition frequency signals, and their pulse modulation rate is a crucial parameter for optimal performance. X-rays with energies exceeding 10 keV can propagate without attenuation in an atmospheric pressure lower than 0.1 Pa. Therefore, high-frequency random-modulated X-ray sources have significant potential applications in deep space communication and interstellar exploration. Additionally, X-ray sources are mainly classified by cathodes as the hot cathode grid-controlled X-ray source (Ma et al., 2014; Feng et al., 2022), the light-controlled X-ray source (Xuan et al., 2021; Cramer et al., 2018), and the cold cathode field emission X-ray source (Yue et al., 2002). Carbon nanotubes (CNTs) are tubular carbon molecules (Choi et al., 2006)used as field emission cathodes in vacuum electronic devices. The number of electrons that are extracted from the cathode is determined by the electric field strength set between the CNT cathode and the grid. The CNT field emission is especially suitable for high-frequency random-modulated X-rays emission due to its fast start-up response and low power consumption (Zhang et al., 2020).

Studies on CNT used for a pulse repetitive electron or X-ray source are abundant, but there are few pieces of research on high-frequency random-modulated X-ray sources with CNT cathodes. For the repetitive source, people generally focus on the large peak current of the CNT cathode. Chen, J.T. et al. (Chen et al., 2017) tested the CNT emitters at 0.4 kHz pulse repetition rate with 10 μs pulse width and a maximum current of 294.7 mA when the grid field is 10.1 V/μm. Zhang, Y. et al. (Zhang et al., 2020) studied the CNT cold cathode in direct current (DC) mode and millisecond pulse mode, and the maximum peak current is 5.06 mA@10.1 V/μm. Yue, G.Z. et al. (Yue et al., 2002) imaged a human extremity by using a CNT cathode pulse X-ray source with 0.5 ms pulse width at 1 kHz pulse repetition rate and tube current density of 100 mA/cm^2 @2.5 V/μm. The pulse repetition rates of electron or X-ray sources are restricted at kHz levels technically due to the CNT cathode's

* Corresponding author. Department of Nuclear Science and Technology, Nanjing University of Aeronautics and Astronautics, Nanjing, 210016, China.
** Corresponding author. Department of Nuclear Science and Technology, Nanjing University of Aeronautics and Astronautics, Nanjing, 210016, China.
E-mail addresses: liuyp@nuaa.edu.cn (Y. Liu), tangxiaobin@nuaa.edu.cn (X. Tang).

https://doi.org/10.1016/j.apradiso.2024.111243
Received 10 May 2023; Received in revised form 1 February 2024; Accepted 18 February 2024
Available online 22 February 2024

pulse power supply technology. For the random X-ray source, the pulse power supply of the CNT cathode also faces great challenges due to the dilemma between the output voltage amplitude and pulse frequency. Specifically, the large output voltage amplitude of the power supply is inversely proportional to the high pulse frequency due to the limitation of the amplification capabilities of components field effect transistors (FETs) (Kuhlicke et al., 2014; Li et al., 2022). Therefore, our previous work (Lai et al., 2021) has proposed a novel voltage loading method on the CNT cathode to achieve as high as 1.05 MHz random pulse X-ray emission. And the anode current is 125 μA, when the grid voltage is 500 V and the corresponding grid field is 2.5 V/μm. However, the grid voltage of 500 V is still high for the cathode's power supply to switch rapidly at frequencies more than 1 MHz. Therefore, this study made an attempt to increase the pulse frequency by lowering the grid voltage on the CNT cathode.

The channel electron multiplier(CEM) is generally a lead glass electron multiplier device (Cramer et al., 2018) with specific secondary electron emission coefficients. It offers high gain, stable performance, a simple structure, and fast response. When a voltage bias is applied on the output of CEM in a vacuum environment, the inner walls of the CEM are capable to release secondary electrons based on the initial electrons emitted by the CNT cathode. The addition of the CEM directly amplifies the current output by the CNT cathode, which offers a chance to relieve the stress of CNT's pulse power supply and realize random pulse X-ray emission at a higher frequency than before.

In this study, a CEM component was attached to the CNT cold cathode triode structure in a vacuum setting. The performances of the developed CNT-CEM X-ray source in direct mode and pulse mode were evaluated and validated through an XCOM transmission experiment. The findings shed light on the potential of utilizing CEM to optimize the pulse voltage supply on CNT, offering a viable solution for achieving higher pulse modulation frequencies of CNT cathode X-ray sources. This work serves as a reference for future research in the XCOM field.

2. System design and measurement method

A CEM component was attached to the CNT triode structure in the dynamic vacuum setting as shown in Fig. 1, and the embedded graphs (a) and (b) present the scanning electron microscopy (SEM) and transmission electron microscopy (TEM) plots, demonstrating the characterization of the CNT cold cathode. The degree of vacuum was always lower than 10^{-5} Pa in the process. The diameter of the CNT cold cathode is 4.88 mm, and square holes with a side length of about 200 μm are used. The lectron transmission rate of the grid can reach to approximately 75%–80% from the cathode according to both CST simulation and experiment for F–N curve. The distance between the cathode and the grid is 200 μm. The entrance area of the CEM is 12.65 mm^2, whose interior is a six-hole helical channel. The distance between the outlet of CEM and the anode is around 1.5 cm. The wires of the components mentioned above including the CNT cathode, grid, CEM, and anode were connected to the external equipment through the electrode flange. The APD detector was used to detect the X-ray signals.

The experiments were conducted in two modes: direct current (DC) and pulse. The only difference in circuit design between the two modes is how the cathode is wired. In DC mode, the cathode was grounded directly to obtain intuitive results of the cathode current generated by the CNT. The results obtained from the DC experiment helped select suitable electronic parameters for the pulse experiments. In pulse mode, the cathode was connected to a power amplifier which amplified the pulse voltages produced by a signal generator, resulting in the formation of groups of pulsed electrons. The electrical field parameters of other components such as the grid, CEM, and anode both in DC and pulse mode were set by the corresponding DC power supplies: the grid voltage ranged from 200 V to 550 V, the CEM bias voltage was 2, 2.2, and 2.5 kV, and the anode voltage was set to 20, 25, and 30 kV, respectively. The cathode current, anode current, and CEM's gain were jointly determined by these electrical parameters. The cathode current was measured directly through the grounded wire by an ammeter, while the anode current was measured by the feedback current of the anode high-voltage power supply. The CEM's gain was calculated as the ratio of the anode current and cathode current, and it was primarily determined by the input current and bias voltage of the CEM. CEM has two electrodes. Maintaining the potential difference of the two electrodes at 2 kV–3 kV results in secondary electrons. Generally, the potential difference between the two electrodes ($\leq$3 kV) affects the secondary electron emission, and the larger the potential difference, the higher the emission.

In pulse mode, the amplitude-frequency response and the X-ray communication performance of the developed CNT-CEM pulse X-ray

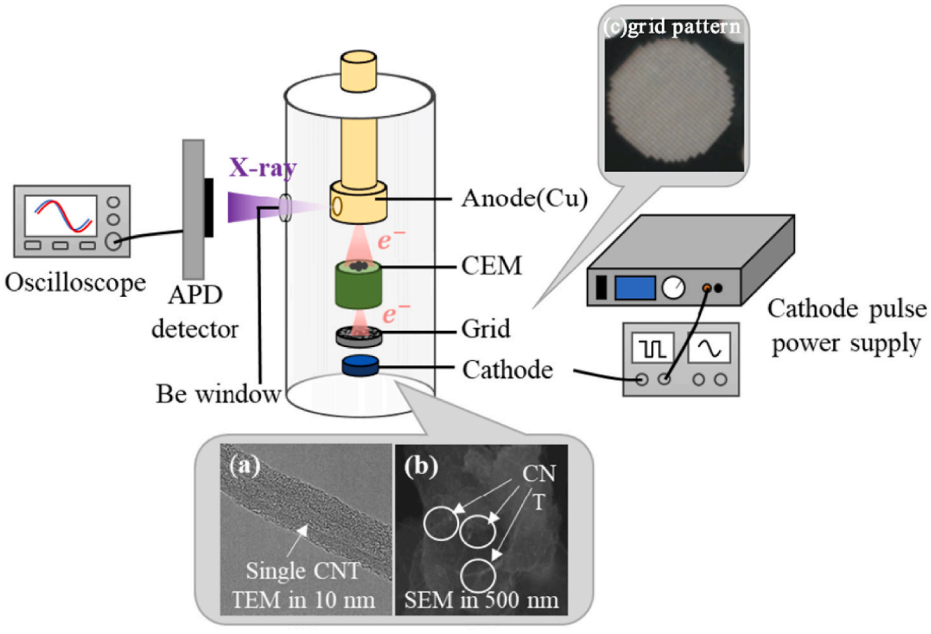

Fig. 1. Structure of the CNT-CEM X-ray source system,
(a) TEM scale in 10 nm and (b) SEM scale in 500 nm (c) grid pattern.

source were tested separately. We used the arbitrary waveform generator (AWG) and the power amplifier to offer pulse voltages on the cathode. The pulse grid voltage between the cathode and the grid caused pulse electron emission. The AWG output modulated pulse voltage waves with the amplitude of 5 V, and then the signals were amplified 10 times by the power amplifier. That means 50 V was used as the pulse voltage difference of the signals of "0" with few X-rays and "1" with many X-rays. For the amplitude-frequency response test, the sinusoidal waves of pulse voltage was applied on the CNT cathode at the frequency range of 1 MHz–6 MHz in order to obtain the 3 dB bandwidth. The pulse X-ray signals from the APD detector and the output voltages from the power amplifier were measured. The normalized amplitude of the X-ray waveform was calculated by the equation of $20\ln(A/B)$ (Lai et al., 2021), where A is the amplitude of the corresponding pulse X-ray signals at different frequencies and B is the maximum value of X-ray signal amplitudes. For the X-ray communication test, the random square waves of pulse voltage was applied on the CNT cathode to produce and then transmit random pulse X-ray signals. The bit-error-rate (BER) is obtained at different communication rates to demonstrate the viability of the pulse CNT-CEM X-ray source.

3. Results and discussion

3.1. System characteristics in DC mode

Fig. 2 shows the anode current and gain at different bias voltages on CEM and anode voltages in the DC mode when the grid voltage is 300 V. As the CEM bias voltage increases from 2.0 kV to 2.5 kV, the anode current and gain generally increase mainly because the CEM bias voltage influences the electric field strength in CEM. When the CEM bias voltage increases, the energy of electrons in the CEM increases, leading to higher secondary emission coefficient (J and B, 1966). Therefore, the multiplied electrons become larger, and as a result, the anode current increases, as shown in Fig. 2(a). Intuitively, the energy of the collision of secondary electrons with the channel walls increases with the bias voltage, thereby increasing the gain, as shown in Fig. 2(b), which is consistent with the results in refs. (J and B, 1966) and (D, 1965). However, for the anode voltage of 25 kV, the gain increases to the maximum at 2.2 kV bias voltage and has a drop at 2.5 kV bias voltage. The gain is determined by many factors such as CEM bias voltage, input current of CEM, and vacuum degree. The drop of the gain is possible due to the slight fluctuation of the vacuum degree during the experiment. As the anode voltages increases from 20 kV to 25 kV, the anode current generally increases mainly because the anode voltage has driven more scattered electrons into the anode. Generally, the influence of the anode voltage on the anode current and gain is not significant and even shows opposite result. For example, the anode current decreases slightly as the anode voltage increases at 2 kV CEM bias voltage. This is possible because the cathode current and the multiplication effect of the CEM are not large enough and have some fluctuations under the relative low CEM bias voltage as well as low grid voltage.

Fig. 3 shows the influence of the grid voltage on the anode current and gain when the CEM bias voltage was set to 2.2 kV. The anode current and the gain of CEM rise rapidly as the grid voltage rises from approximate 230 V–290 V. The gain of CEM shows its best performance of amplifying the cathode current at those range of grid voltage. When the grid voltage is larger than 290 V, the gain begins to decrease as the grid voltage increases, thereby slowing down the increase in the anode current. On the one hand, the decrease in the gain is due to the saturation of the CEM output current caused by the space charge effect. The electrons including scattered electrons and true secondary electrons are more and more accumulated from the inlet end to the outlet end of the CEM. These electrons form the electron cloud, which is much denser at the direction of the outlet end (Xu et al., 2017). The electron cloud will inhibit secondary electrons from further emitting from the channel walls. On the other hand, the channel wall charging and high resistance also contribute to the decrease in the gain (Giudicotti, 2002, 2011). With the high resistance value of CEM, the channel walls cannot charge rapidly

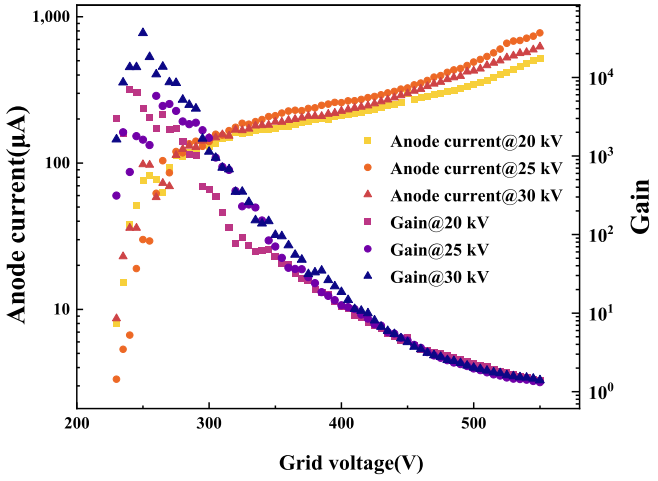

Fig. 3. Anode current and gain of different grid voltages and anode voltages under 2.2 kV bias voltage on CEM.

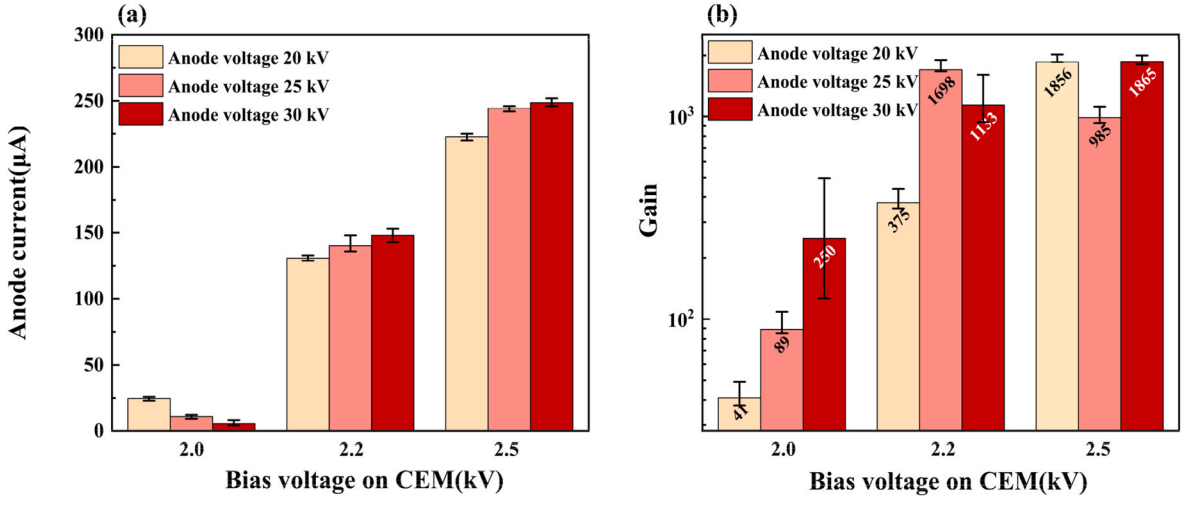

Fig. 2. (a) Anode current and (b) gain at different bias voltages on CEM and anode voltages in the DC mode under the grid voltage of 300 V.

when the electrons are released.

Fig. 4(a) shows the *I–V* curve of the CNT-CEM X-ray source. The cathode current increases exponentially as the grid voltage increases. During the Fowler–Nordheim (F–N) theoretical verification, the cathode current was used to calculate the current density, *J*. In Fig. 4(b), $\ln(J/E^2)$ and $1/E$ show a linear relationship according to the F–N formula, and the R-squared values of these linear fitting at 20 kV, 25 kV and 30 kV are 0.9900, 0.9790 and 0.9857. Those results indicate that the cathode electron emission belongs to field emission type. As shown in Fig. 4(a), the grid voltage required to achieve the same anode current is clearly lower with the addition of the CEM on the CNT cathode. At the condition of 2.2 kV CEM bias voltage and 25 kV anode voltage, the anode currents are 141, 250, and 300 μA at 290, 387.6, and 432.2 V grid voltage, respectively, and the corresponding grid field values are 1.45, 1.94, and 2.16 V/μm. When the anode voltage rises to 30 kV, the grid field is 1.50 V/μm at the anode current of 250 μA. CEM does work for reducing the grid voltage as well as the corresponding grid field strength obviously, although it doesn't achieve a magnitude reduction. The main reason is the mismatching between the output area of CNT and the input area of CEM. Only small part of electrons emitted from the cathode enter into the CEM and bombards the anode target to produce pulsed X-rays.

3.2. X-ray pulse emission characteristics

Based on the test results in DC mode in Fig. 3, the anode current has a sharp rise at low grid voltage from 230 V to 290 V. This range is suitable for distinguishing the intensity variation of the modulated pulse X-ray signals. Therefore, the grid voltages with the range of 230 V–290 V were employed in pulse mode. The CEM bias voltage and anode voltage were set to 2.2 kV and 25 kV, respectively.

Fig. 5(a) shows the sinusoidal waveforms of the power amplifier and X-ray signals for the CEM-CNT X-ray source at frequencies ranging from 1 MHz to 6 MHz. Accordingly, the amplitude-frequency responses were obtained at grid voltages of 250, 270, and 290 V, respectively. When the frequency increases, the width of single pulse decreases, and the number of the detected X-rays in one single pulse decreases accordingly. As a result, the waveform spikes become more evident in Fig. 5(a), and the X-ray amplitude decreases in Fig. 5(b). The grid voltage also affects the amplitude of X-ray signals. The normalized X-ray amplitude at −3 dB corresponds to a bandwidth of 3.28 MHz for 250 V grid voltage, 3.57 MHz for 270 V, and 3.58 MHz for 290 V. Compared to our previous work (Lai et al., 2021), 3 dB bandwidth of the CNT pulse X-ray source with adding the CEM increases from 1.05 MHz to 3.58 MHz, and the grid field decreases from 2.5 V/μm to 1.45 V/μm. The results prove that the CNT-CEM X-ray source achieves higher frequency and lower grid voltage when the same anode current is maintained. This finding lays a foundation for wider applications of CNT cathode pulse X-ray sources.

3.3. Application in X-ray communication

During the XCOM experiment, the pseudo-random code PRBS7 was used, and 200,000 bits were sampled offline for demodulation to obtain the BER at different communication rates from 1 Mbps to 6 Mbps. The X-rays are too particle-like. Counting this deviation in waveform amplitude is of little significance from an application point of view. Relaying on that, we believe that if the detector and its circuit can distinguish the "1″ signal of the X-rays, it is considered to be stable. During the communication experiment, the bias voltage on CEM was 2.2 kV, the anode voltage was 25 kV, and the grid voltage was 290 V. Fig. 6 exhibits the square waveforms of the power amplifier's output voltage and the detected X-ray signals. The values of the BER are 0 at 1 Mbps, 5.34×10^{-5} at 2 Mbps, 3.55×10^{-5} at 3 Mbps, and 1.10×10^{-3} at 6 Mbps, respectively. That means the developed CNT-CEM pulse X-ray source could support at least 6 Mbps X-ray communication. The increase in BER is caused by the decrease in the signal density of one pulse X-ray as the communication rate increases.

4. Conclusion

This study proposed a high-frequency pulse X-ray source, which combines a CNT cold cathode with a CEM, and tested its DC and pulse emission characteristics. Results suggest that the CNT-CEM X-ray source breaks the frequency limit resulting from the power supply technology, and realizes high-frequency random pulse emission under low grid voltage. In the DC mode, under the conditions of 2.2 kV CEM bias voltage and 25 kV anode voltage, the anode currents are 141, 250, and 300 μA at grid voltages of 290, 387.6, and 432.2 V; the corresponding grid field values are 1.45, 1.94, and 2.16 V/μm, respectively. In the pulse mode, the amplitude-frequency response of the developed CNT-CEM X-ray source were tested. The 3 dB bandwidth is 3.28 MHz for 250 V grid voltage, 3.57 MHz for 270 V, and 3.58 MHz for 290 V, respectively. In addition, the developed pulse X-ray source was introduced into the X-ray communication. The experimental communication rate reaches 6 Mbps with the BER of 1.1×10^{-3}. The developed high-frequency pulse CNT-CEM X-ray source has potential applications in XCOM, high-speed X-ray imaging, and other fields.

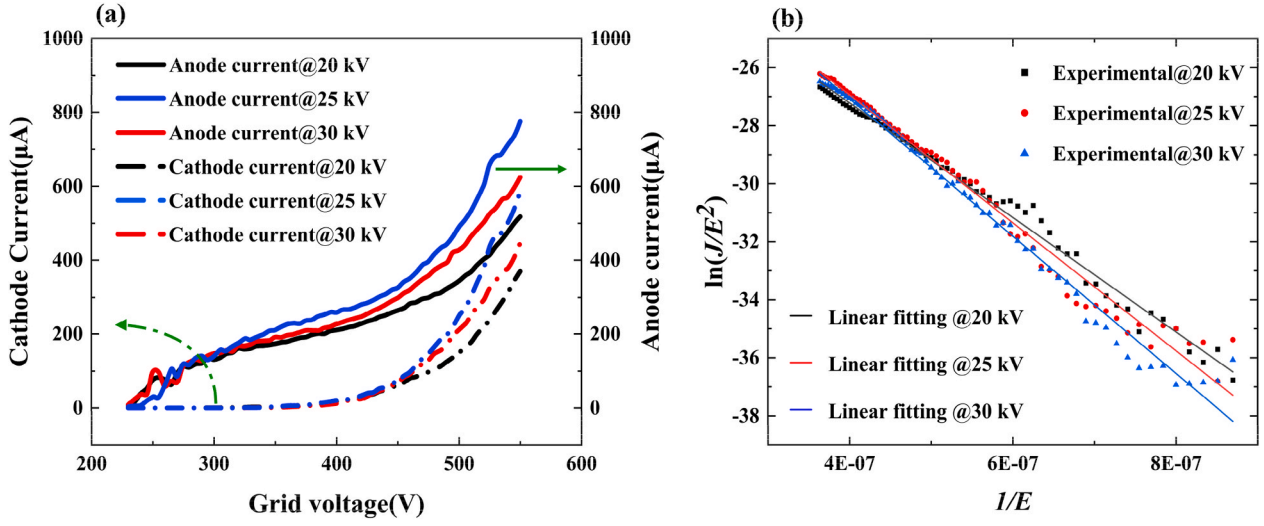

Fig. 4. (a) *I–V* curve and (b) F–N theoretical verification of the CNT-CEM X-ray source at different anode voltages under 2.2 kV CEM bias voltage on CEM.

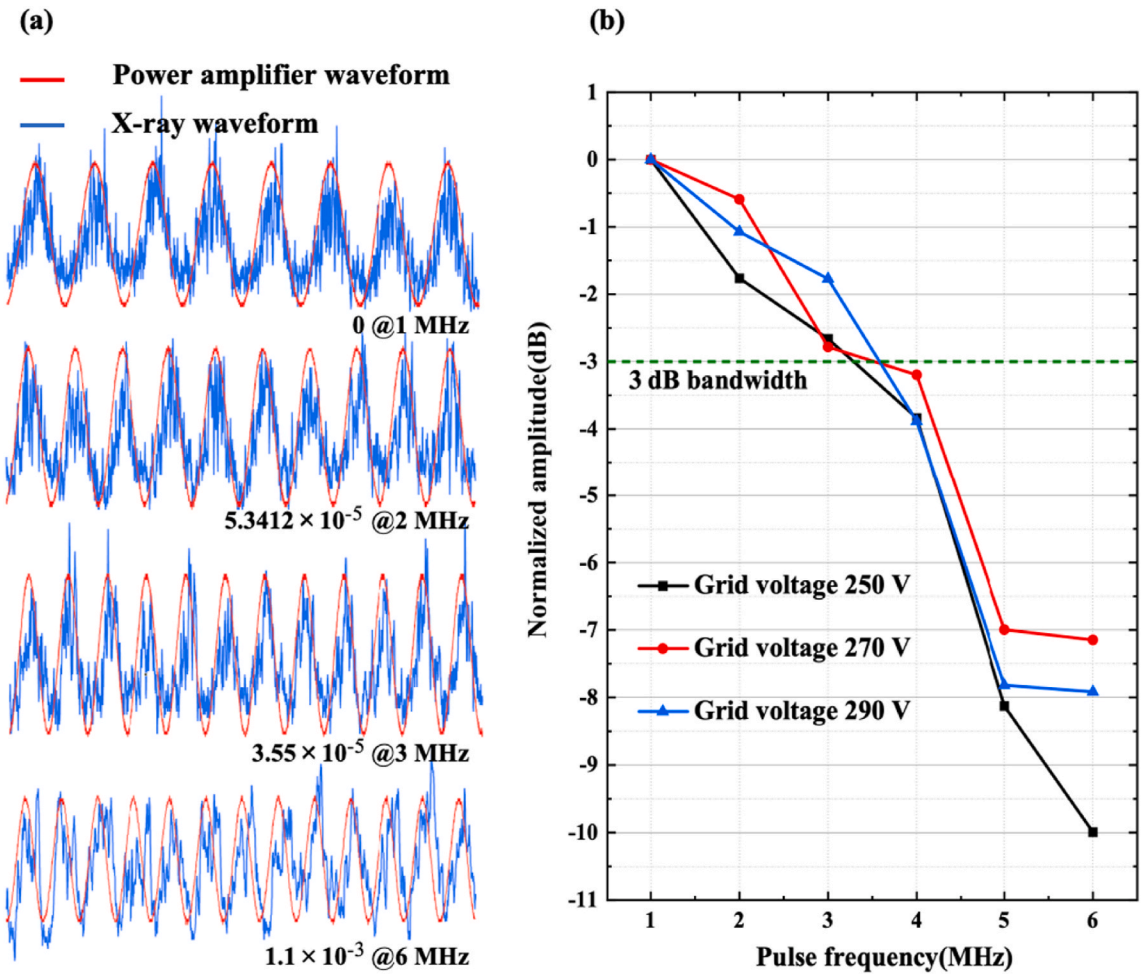

Fig. 5. Pulse characteristics including (a) waveforms and (b) amplitude-frequency response of the CEM-CNT X-ray source at different grid voltages under 2.2 kV CEM bias voltage and 25 kV anode voltage.

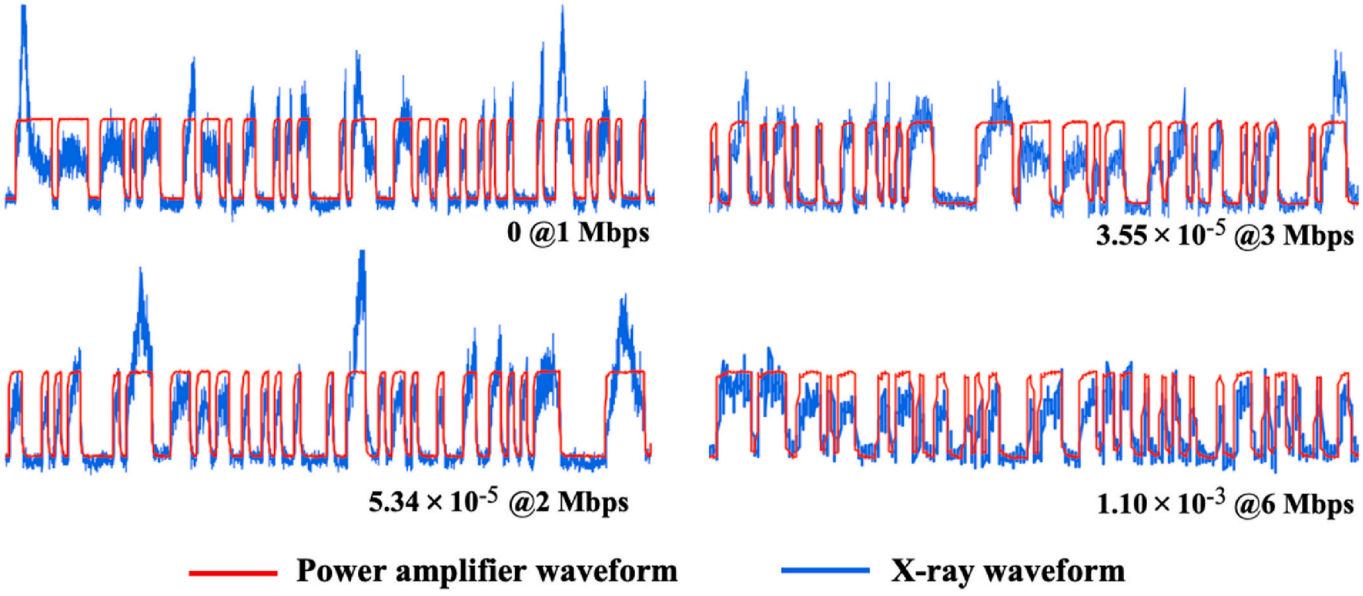

Fig. 6. Waveforms and BER of XCOM experiment.

CRediT authorship contribution statement

Kai Miao: Writing – original draft, Methodology, Investigation, Formal analysis, Data curation. **Yunpeng Liu:** Writing – review & editing, Resources, Conceptualization. **Sheng Lai:** Writing – review & editing, Formal analysis. **Junqiu Yin:** Writing – review & editing, Formal analysis. **Feixu Xiong:** Writing – review & editing, Formal analysis. **Xiaoyu Dong:** Resources. **Xiaobin Tang:** Writing – review & editing, Resources, Conceptualization.

Declaration of competing interest

The authors declare the following financial interests/personal relationships which may be considered as potential competing interests: Yunpeng Liu reports financial support was provided by National Natural Science Foundation of China. If there are other authors, they declare that they have no known competing financial interests or personal relationships that could have appeared to influence the work reported in this paper.

Data availability

Data will be made available on request.

Acknowledgment

This work was supported by the National Natural Science Foundation of China (Grant No. 12375256) and the Fundamental Research Funds for the Central Universities (Grant No. NT2023012).

References

Chen, J.T., Yang, B.J., Liu, X.H., Yang, J., Cui, L.F., Yan, X.B., 2017. Large field emission current and density from robust carbon nanotube cathodes for continuous and pulsed electron sources. Sci. China Mater. 60, 335–342.

Choi, H.Y., Chang, W.S., Kim, H.S., Park, Y.H., Kim, J.U., 2006. Acquisition of X-ray images by using a CNT cold emitter. Phys. Lett. 357, 36–41.

Cramer, A., Hecla, J., Wu, D.F., Lai, X.C., Boers, T., Yang, K., Moulton, T., Kenyon, S., Arzoumanian, Z., Krull, W., Gendreau, K., Gupta, R., 2018. Stationary Computed tomography for space and other resource-constrained environments. SCI REP-UK 8.

D, S.E., 1965. Low energy charged particle detection using the continuous channel electron multiplier. IEEE T NUCL SCI 12, 34–38.

Feng, Z., Liu, Y., Mu, J., Chen, W., Lai, S., Tang, X., 2022. Optimization and testing of groove-shaped grid-controlled modulated X-ray tube for X-ray communication. Nucl. Instrum. Methods Phys. Res. Sect. A Accel. Spectrom. Detect. Assoc. Equip. 1026, 166218.

Giudicotti, L., 2002. Analytical, steady-state model of gain saturation in channel electron multipliers. Nucl. Instrum. Methods Phys. Res. Sect. A Accel. Spectrom. Detect. Assoc. Equip. 480, 670–679.

Giudicotti, L., 2011. Time dependent model of gain saturation in microchannel plates and channel electron multipliers. Nucl. Instrum. Methods Phys. Res. Sect. A Accel. Spectrom. Detect. Assoc. Equip. 659, 336–347.

J, A., B, W.M., 1966. The mechanism of channel electron multiplication. IEEE T NUCL SCI 13, 88–99.

Kuhlicke, A., Palis, K., Benson, O., 2014. Broadband linear high-voltage amplifier for radio frequency ion traps. Rev. Sci. Instrum. 85, 114707.

Lai, S., Tang, X., Liu, Y., Mu, J., Feng, Z., Miao, K., 2021. X-ray high frequency pulse emission characteristic and application of CNT cold cathode x-ray source cathode x-ray source. Nanotechnology 33, 075201.

Li, Y., Chen, G., Zhao, S., Liu, C., Zhao, N., 2022. Addressing gain-bandwidth trade-off by a monolithically integrated photovoltaic transistor. Sci. Adv. 8, eabq0187.

Ma, X.F., Zhao, B.S., Sheng, L.Z., Liu, Y.A., Liu, D., Deng, N.Q., 2014. Grid-controlled emission source for space X-ray communication. Acta Phys. Sin-CH ED 63.

Xu, Y.L., Xu, T., Liu, H., Cai, H., Wang, C.L., 2017. Gain regulation of the microchannel plate system. Int. J. Mass Spectrom. 421, 234–237.

Xuan, H., Liu, Y., Qiang, P., Su, T., Yang, X., Sheng, L., Zhao, B., 2021. Light-controlled pulsed x-ray tube with photocathode. Chin. Phys. B 30, 118502.

Yue, G.Z., Qiu, Q., Gao, B., Cheng, Y., Zhang, J., Shimoda, H., Chang, S., Lu, J.P., Zhou, O., 2002. Generation of continuous and pulsed diagnostic imaging x-ray radiation using a carbon-nanotube-based field-emission cathode. Appl. Phys. Lett. 81, 355–357.

Zhang, Y., Tan, Y., Wang, L., Li, B., Ke, Y., Liao, M., Xu, N., Chen, J., Deng, S., 2020. Electron emission and structure stability of carbon nanotube cold cathode driven by millisecond pulsed voltage. Vacuum 172, 109071.